DOI: 10.1002/ejic.200700735

# Hierarchical Structures in Tin(II) Oxalates

Padmini Ramaswamy,[a] Ayan Datta,[b] and Srinivasan Natarajan*[a]

**Keywords:** Template synthesis / Lone pair / Hydrogen bonds / Tin / Oxalate

Six new $Sn^{II}$ oxalates exhibiting a hierarchy of structures have been prepared employing hydrothermal methods. The compounds **I** $[C_{10}N_2H_{10}][Sn(C_2O_4)_2]$, **II** $[C_{10}N_2H_{10}][Sn_2(C_2O_4)_3]$, and **III** $[C_8N_4H_{26}][Sn(C_2O_4)_2]_2{\cdot}2H_2O$ possess zero-dimensional molecular structures; **IV** $[C_{10}N_2H_8]_2[Sn(C_2O_4)]_2$ and **V** $[C_{12}N_2H_8][SnC_2O_4]$ have one-dimensional chain structures; and compound **VI** $[C_5N_2H_{14}]_2[Sn_4(C_2O_4)_6]{\cdot}7H_2O$ has a two-dimensional layer structure. The $Sn^{II}$ ions have 4- and 6-coordination with square-pyramidal or pentagonal-bipyramidal geometry, in which the lone pair of electrons also occupies one of the vertices. Weak intermolecular forces such as hydrogen-bond interactions, π···π interactions, and lone-pair–π interactions have been observed and appear to lend structural stability. Theoretical studies indicate that the π···π interaction energy between the bound 1,10-phenanthroline molecules is of the order of 5–6 kcal mol$^{-1}$ in **V**. Natural bond orbital (NBO) analysis on two model compounds, **II** and **IV**, indicates reasonable lone-pair–π interactions. The close structural relationship between all the compounds indicates that a building-up process from the zero-dimensional monomer can be considered. The present structures provide opportunities for evaluating the structure-directing role of the lone pair of electrons of $Sn^{II}$.



## Introduction

Compounds possessing extended network structures continue to be of interest for their many applications, in the areas of catalysis, sorption, and separation processes.[1] Though the literature abounds with examples of the synthesis of solids based on tetrahedral or octahedral–tetrahedral networks, there is considerable interest in the study of compounds based on inorganic–organic hybrids as well.[2,3] These are compounds based on dicarboxylates, which exhibit properties that combine the inherent porosity with the functionality of the organic linkers. Thus, gas sorption, luminescence, and catalytic behavior have been observed in many carboxylates.[3] Of these, the oxalates are a special class of dicarboxylates. Oxalate-based compounds, especially those of transition elements, have been studied extensively for their interesting magnetic properties.[4,5] For example, mixed metal oxalates, $A[M^{II}M^{III}(ox)_3]$ (A = monocation; $M^{II}$ = Mn, Fe, Co, Ni, Cu, Zn; $M^{III}$ = Cr, Fe, Co), exhibit magnetic properties that vary from simple paramagnetic to ferromagnetic or antiferromagnetic.[6] In addition, it has been established that the oxalates are good precursors for the preparation of complex metal oxides such as barium titanate.[7] Recently, it has been shown that amine-templated oxalate compounds with open-framework structures can be prepared employing novel approaches.[8] One of the important developments in the area of open-framework solids is the use of hydrogen-bonded adducts, formed between the organic amine and the participating acid, as the starting material. This approach, in fact, gives rise to open-framework structures much more readily and at temperatures that are lower than those normally employed.[9,10] It has been shown that the use of amine-oxalates along with a suitable metal ion can give rise to interesting structures.[8,11] A combination of this and the conventional hydrothermal process has given rise to a variety of framework oxalates. Thus, open-framework oxalates based on Zn,[8] Cd,[12] Y,[13] Nd,[14] La,[15] and Sn[16–18] have been prepared and characterized. Of these, we have been interested in the study of $Sn^{II}$ oxalates. The $Sn^{II}$ oxalates exhibit zero-,[16] one-,[17] and two-dimensionally[18] extended network structures.

In the $Sn^{II}$ oxalates, the $Sn^{II}$ atoms are, in general, coordinated with four or six oxygen atoms, but the resulting geometries around the central $Sn^{II}$ are considerably distorted because of the presence of a lone pair of electrons associated with the $Sn^{II}$. Furthermore, the lone pair appears to play an important role in the formation of these structures. In order to understand the role of the lone pair of electrons of $Sn^{II}$, it is important to synthesize a large number of $Sn^{II}$-based compounds. We have therefore been studying the reactivity of $Sn^{II}$ salts under hydrothermal conditions.[18] During the course of this study, we have now prepared a series of tin(II) oxalates, exhibiting a hierarchy of structures in the presence of a variety of organic amines.

[a] Framework Solids Laboratory, Solid State and Structural Chemistry Unit, Indian Institute of Science, Bangalore 560012, India
E-mail: snatarajan@sscu.iisc.ernet.in
[b] Chemistry and Physics of Materials Unit, Jawaharlal Nehru Centre for Advanced Scientific Research, Jakkur, Bangalore 560064, India

Supporting information for this article is available on the WWW under http://www.eurjic.org or from the author.

  

The compounds $[C_{10}N_2H_{10}][Sn(C_2O_4)_2]$ (**I**), $[C_{10}N_2H_{10}]$-$[Sn_2(C_2O_4)_3]$ (**II**), $[C_8N_4H_{26}][Sn(C_2O_4)_2]_2{\cdot}2H_2O$ (**III**), $[C_{10}N_2H_8]_2[Sn(C_2O_4)]_2$ (**IV**), $[C_{12}N_2H_8][SnC_2O_4]$ (**V**), and $[C_5N_2H_{14}]_2[Sn_4(C_2O_4)_6]{\cdot}7H_2O$ (**VI**) have been obtained by hydrothermal methods. These possess zero- (**I**, **II**, and **III**), one- (**IV** and **V**), and two- (**VI**) dimensional structures.

## Results and Discussion

### Zero-Dimensional Structures: $[C_{10}N_2H_{10}][Sn(C_2O_4)_2]$ (I), $[C_{10}N_2H_{10}][Sn_2(C_2O_4)_3]$ (II), and $[C_8N_4H_{26}][Sn(C_2O_4)_2]_2{\cdot}2H_2O$ (III)

The three zero-dimensional compounds, **I**–**III**, were prepared using the hydrothermal method. The use of $H_3PO_4$ appears to be necessary for the formation of **I**, whereas both $H_2C_2O_4$ and $H_3PO_4$ are needed for isolating **III**, both of which have a simple monomeric tin(II) oxalate unit. The compound **II**, which is a dimeric tin(II) oxalate, forms without the use of any additional acids in the reaction mixture. The asymmetric units of **I**, **II**, and **III** consist of 13, 22, and 20 non-hydrogen atoms respectively. In all three compounds, the $Sn^{II}$ atom appears to have 4-coordination with respect to the oxalate oxygen atoms, and the presence of the lone pair of electrons makes it approximately 5-coordinate, as the lone pair of electrons is expected to occupy one of the vertices of the coordination geometry around the central metal atom. Thus, for a 5-coordinate system, there are two possible geometries: square-pyramidal and trigonal-bipyramidal.[19] A careful analysis of the observed bond lengths in each case clearly indicates that in all three compounds we have a distorted square-pyramidal arrangement. The degree of distortion varies significantly. For compound **I**, the Sn–O distances are in the range 2.138(2)–2.296(2) Å (av. 2.217 Å) and the O–Sn–O bond angles are in the range 73.60(8)–141.52(11)° (av. 89.16°); for compound **II**, the Sn–O bond lengths are in the range 2.153(2)–2.359(2) Å (av. 2.233 Å) and the O–Sn–O bond angles are in the range 72.16(5)–136.04(6)° (av. 88.51°); and for **III**, the Sn–O bond lengths are in the range 2.174(2)–2.376(2) Å (av. 2.258 Å) and the O–Sn–O bond angles are in the range 72.06(6)–146.44(6)° (av. 89.61°) (Table S1). The O–Sn–O bond angles are closer to the value of O–Sn–O bond angles and distances observed for $Sn^{II}O$, where $Sn^{II}$ exists in a square-pyramidal geometry with respect to the oxygen atoms.[20] Similar coordination geometries have been observed before.[16] In all the compounds, the $SnO_4$ units are connected to the carbon atoms forming the observed monomeric $Sn^{II}$ oxalate units in **I** and **III** and a dimeric unit in **II**, all of which are anionic. The charge compensation is achieved by the presence of protonated organic amine cations in all three structures. Thus, in **I** and **II** we have 4,4′-bpy and in **III** BAPEN molecules, which occupy spaces in between the $Sn^{II}$ oxalate molecular units. The presence of anionic and cationic species in close proximity gives rise to significant hydrogen-bond interactions (Table 1), which lead to a supramolecularly extended layer-like arrangement in all three compounds (Figure 1, a–c).

Table 1. Important hydrogen-bond interactions (distances given in Å) for compounds **I**–**VI**.

| D–H···A | D–H | H···A | D···A | D–H···A |
|---|---|---|---|---|
| **I** | | | | |
| N(1)–H(1)···O(4) | 0.86 | 1.87 | 2.674(4) | 154 |
| C(23)–H(23)···O(1) | 0.93 | 2.36 | 3.270(4) | 166 |
| C(21)–H(21)···O(1) | 0.93 | 2.60 | 3.523(5) | 173 |
| C(22)–H(22)···O(2) | 0.93 | 2.34 | 3.208(5) | 155 |
| **II** | | | | |
| N(1)–H(1)···O(6) | 0.86 | 1.97 | 2.743(3) | 149 |
| C(21)–H(21)···O(3) | 0.93 | 2.34 | 3.216(3) | 156 |
| C(23)–H(23)···O(4) | 0.93 | 2.45 | 3.377(3) | 174 |
| **III** | | | | |
| N(1)–H(3)···O(100) | 0.89 | 2.16 | 2.962(3) | 150 |
| N(2)–H(10)···O(5) | 0.90 | 1.96 | 2.854(3) | 174 |
| N(2)–H(11)···O(6) | 0.90 | 1.95 | 2.848(2) | 172 |
| O(100)–H(102)···O(8) | 0.85 | 2.23 | 3.055(4) | 164 |
| C(11)–H(9)···O(7) | 0.97 | 2.51 | 3.388(3) | 150 |
| **VI** | | | | |
| N(4)–H(16)···O(5) | 0.90 | 2.60 | 3.475(17) | 166 |
| C(30)–H(7)···O(300) | 0.97 | 1.82 | 2.762(9) | 164 |
| C(32)–H(9)···O(16) | 0.97 | 2.38 | 3.317(8) | 162 |
| C(34)–H (11)···O(600) | 0.97 | 1.82 | 2.767(8) | 163 |
| C(34)–H(12)···O(18) | 0.97 | 1.85 | 2.811(7) | 173 |
| C(39)–H(22)···O(13) | 0.97 | 2.24 | 3.164(11) | 159 |
| C(35)–H(20)···O(700) | 0.97 | 2.56 | 3.435(17) | 150 |
| C(38)–H(23)···O(3) | 0.97 | 1.93 | 2.845(10) | 156 |
| C(38)–H(24)···O(500) | 0.97 | 1.90 | 2.839(14) | 163 |

It can be seen from the packing diagram that in **I** the $Sn^{II}$ oxalates and the 4,4′-bipy units strictly alternate, while in **II** and **III** the oxalate units form one-dimensional tapes, which are separated by the organic amine molecules. In addition, we also observe that the 4,4′-bpy units in **II** are twisted around the central C–C bond with an average torsion angle of 121.2°. The twisting of the 4,4′-bpy also appears to coincide with the bending of the $Sn^{II}$ oxalate units, presumably to maximize the hydrogen-bond interactions between the anions and the cations. The coordination geometry around the $Sn^{II}$ ions and the structural arrangement indicate active participation of the stereo-active lone pair of electrons of $Sn^{II}$. Similar structural arrangements have been noted earlier.[16]

The role and importance of hydrogen-bond interactions in open-framework structures have been discussed before.[8,11] In **I**–**III**, we have both N–H.O and C–H···O interactions. The N···O (donor–acceptor) distances are in the range 2.674(4)–3.475(2) Å (av. 2.674 Å for **I**, 2.743 Å for **II**, and 2.888 Å for **III**) and the N–H···O bond angles are in the range 149.0–174.0° (av. 154.0° for **I**, 149.0° for **II**, and 165.3° for **III**) (Table S1). Similarly, the C···O distances are in the range 2.767(8)–3.523(5) Å (av. 3.334 Å for **I**, 3.297 Å for **II**, and 3.388 Å for **III**) while the C–H···O bond angles are in the range 150–173° (av. 164.7° for **I**, 165° for **II**, and 150° for **III**). From the N···O and C···O distances, it is clear that the N–H···O interactions are stronger than the C–H···O interactions (Figure S10). It has been argued that the C–H···O interactions can provide structural support by

  

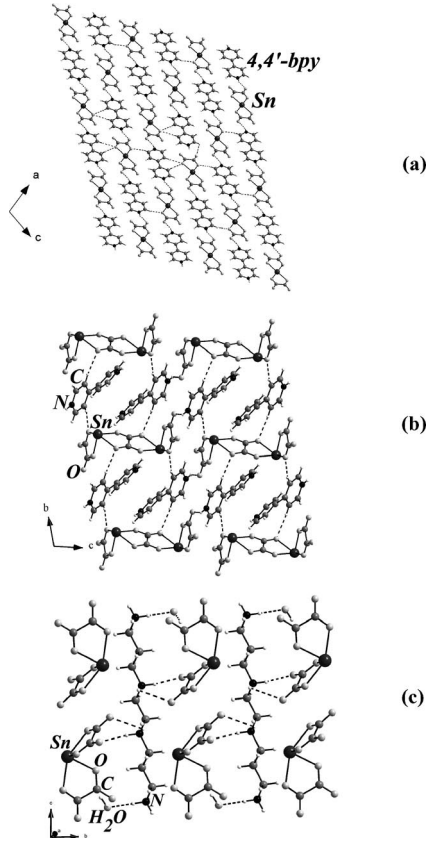


Figure 1. The packing diagram showing the arrangement of $Sn^{II}$ oxalate and the amine molecules in (a) $[C_{10}N_2H_{10}][Sn(C_2O_4)_2]$ (**I**), (b) $[C_{10}N_2H_{10}][Sn_2(C_2O_4)_3]$ (**II**), and (c) $[C_8N_4H_{26}][Sn(C_2O_4)_2]_2 \cdot 2H_2O$ (**III**).

playing an active secondary role and also act as important "steering forces" in solid-state assemblies.[21] It has been shown that in the absence of stronger intermolecular interactions, weak hydrogen bonds can be employed gainfully to direct the crystal design. In our present compounds **I**–**III**, the hydrogen-bond interactions are significant and comparable to the values normally encountered in organic solids.[22]

### One-Dimensional Structures: $[C_{10}N_2H_8]_2[Sn(C_2O_4)]_2$ (IV) and $[C_{12}N_2H_8][SnC_2O_4]$ (V)

The two one-dimensional compounds **IV** and **V** were obtained through a hydrothermal process. We have been able to synthesize the pure single phasic compound of **V** both at low (150 °C/48 h) and high temperatures (150 °C/48 h + 180 °C/24 h). A similar approach, however, did not result in a pure phase of **IV**, indicating the unpredictability of the kinetically controlled processes under hydrothermal conditions.

The asymmetric units of **IV** and **V** contain 38 and 21 non-hydrogen atoms, respectively. Of these, two tin atoms in **IV** and one tin atom in **V** are crystallographically independent. The Sn atoms in **IV** have two different coordination environments. Thus Sn(1) is coordinated by four oxygen atoms and Sn(2) by four oxygen and two nitrogen atoms. In **V**, the Sn atoms are coordinated by four oxygen and two nitrogen atoms only. The Sn–O bond lengths are in the range 2.169(3)–2.472(3) Å (av. 2.314 Å) for **IV** and in the range 2.146(2)–2.535(2) Å (av. 2.380 Å) for **V**. The Sn–N bond lengths are in the range 2.491(3)–2.533(4) Å (av. 2.512 Å) for **IV** and in the range 2.612(2)–2.613(2) Å (av. 2.6125 Å) for **V**. The O/N–Sn–O/N bond angles are in the range 64.80(11)–136.62(10)° (av. 90.3°) for **IV** and in the range 62.77(6)–154.89(6)° (av. 96.2°) for **V** (Table S1).

The coordination geometry around the $Sn^{II}$ atoms presents two distinct units (Figure 2, a). The 4-coordinated $Sn^{II}$ atoms [Sn(1)] have a distorted square-pyramidal arrangement with four oxygen atoms in the plane and the vertex being occupied by the lone pair of electrons, similar to that observed for compounds **I**–**III**. The 6-coordinated $Sn^{II}$ atoms have three oxygen and two nitrogen atoms in a plane forming a pentagon, with the other oxygen atom along with the lone pair of electrons forming the two vertices, above and below the plane of the pentagon, giving rise to a pseudopentagonal bipyramidal arrangement. This coordination geometry around the hexacoordinate $Sn^{II}$ resembles the 14-electron species observed in interhalogen compounds such as $[IF_6]^-$. Similar coordination environments for $Sn^{II}$ have been observed in the tin oxalate structures reported previously.[16,18]

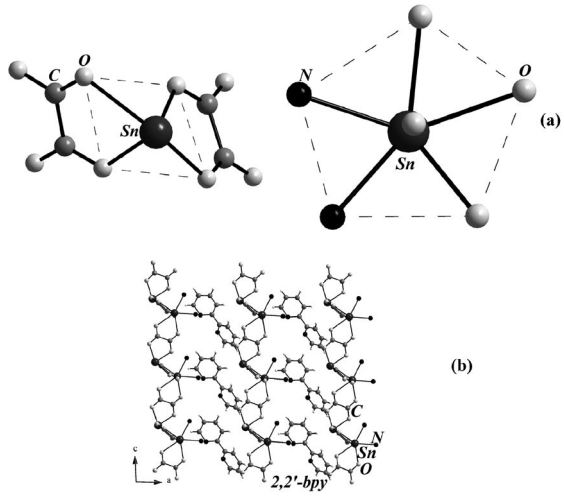


Figure 2. (a) The coordination environment around $Sn^{II}$ ions in $[C_{10}N_2H_8]_2[Sn(C_2O_4)]_2$ (**IV**). The lone pair in both the cases occupies the other vertex (see text). (b) Structure of **IV** in the *ac* plane, showing the arrangement of chains. The bound 2,2′-bpy molecule is not shown for clarity. Note that the interchain spaces are occupied by the twisted 2,2′-bpy molecule.

The Sn atoms are connected to the oxalate units through the Sn–O–C bonds, and with the 2,2′-bipyridine and the 1,10-phenanthroline ligands through Sn–N–C linkages. The C–O, C–N, and C–C bond lengths are in the ranges expected for this bonding. Selected bond lengths are listed in Table 2.

  

Table 2. Selected bond lengths (Å) for compounds **I**–**VI**.[a]

| Bond | Length | Bond | Length |
|---|---|---|---|
| Compound **I** | | | |
| Sn(1)–O(1) | 2.2960(2) | Sn(1)–O(2) | 2.1380(2) |
| Sn(1)–O(1)#1 | 2.2960(2) | Sn(1)–O(2)#1 | 2.1380(2) |
| Compound **II** | | | |
| Sn(1)–O(1) | 2.1533(16) | Sn(1)–O(3) | 2.2305(16) |
| Sn(1)–O(2) | 2.1894(16) | Sn(1)–O(4) | 2.3588(15) |
| Compound **III** | | | |
| Sn(1)–O(1) | 2.1744(16) | Sn(1)–O(3) | 2.2510(16) |
| Sn(1)–O(2) | 2.2307(16) | Sn(1)–O(4) | 2.3755(19) |
| Compound **IV** | | | |
| Sn(1)–O(1) | 2.1790 (3) | Sn(2)–O(6) | 2.4580(3) |
| Sn(1)–O(2) | 2.2270(3) | Sn(2)–O(7)#1 | 2.4600(3) |
| Sn(1)–O(3) | 2.2350(3) | Sn(2)–(O8) | 2.617(3) |
| Sn(1)–O(4) | 2.4720(3) | Sn(2)–N(1) | 2.4910(3) |
| Sn(2)–O(5)#1 | 2.1690(3) | Sn(2)–N(2) | 2.5330(4) |
| Compound **V** | | | |
| Sn(1)–O(1) | 2.1462(16) | Sn(1)–O(4) | 2.5352(18) |
| Sn(1)–O(2)#1 | 2.3535(17) | Sn(1)–N(1) | 2.6130(2) |
| Sn(1)–O(3) | 2.4852(17) | Sn(1)–N(2) | 2.6120(2) |
| Compound **VI** | | | |
| Sn(1)–O(1) | 2.1720(5) | Sn(3)–O(13) | 2.1660(5) |
| Sn(1)–O(2) | 2.3790(5) | Sn(3)–O(14) | 2.3410(5) |
| Sn(1)–O(3) | 2.3850(5) | Sn(3)–O(15) | 2.4160(5) |
| Sn(1)–O(4) | 2.4490(5) | Sn(3)–O(16) | 2.4760(5) |
| Sn(1)–O(5) | 2.4950(5) | Sn(3)–O(17) | 2.4850(5) |
| Sn(1)–O(6) | 2.5410(5) | Sn(3)–O(18) | 2.5120(5) |
| Sn(2)–O(7) | 2.1730(5) | Sn(4)–O(19) | 2.1600(5) |
| Sn(2)–O(8) | 2.3310(5) | Sn(4)–O(20) | 2.3230(5) |
| Sn(2)–O(9) | 2.4480(5) | Sn(4)–O(21) | 2.4000(5) |
| Sn(2)–O(10) | 2.4650(5) | Sn(4)–O(22) | 2.4790(5) |
| Sn(2)–O(11) | 2.5000(5) | Sn(4)–O(23) | 2.4990(5) |
| Sn(2)–O(12) | 2.5460(5) | Sn(4)–O(24) | 2.5030(5) |

[a] Symmetry transformations used to generate equivalent atoms. For compound **I**: #1 $-x + 1$, $y$, $-z + 3/2$; for compound **III**: #1 $-x + 2$, $-y$, $-z + 1$; for compound **IV**: #1 $x$, $-y + 3/2$, $z - 1/2$; for compound **V**: #1 $x$, $-y + 3/2$, $z - 1/2$; for compound **VI**: #1 $x$, $-y + 1/2$, $z + 1/2$.

In the structure of **IV**, the $SnO_4$ units and the $SnO_4N_2$ units alternate along the chain and are connected through the carbon atoms forming a neutral one-dimensional $Sn^{II}$ oxalate structure. There are two different 2,2′-bpy units in the structure. While one of the 2,2′-bpy units is bound to the $Sn^{II}$ through the Sn–N bond, the other neutral 2,2′-bpy unit occupies the interchain spaces (Figure 2, b). This free 2,2′-bpy molecule is not planar, but twisted around the central C–C bond with an average torsion angle of 118.9°. In **V**, the connectivity between the $SnO_4N_2$ units (Figure 3, a) and the carbon atoms forms a neutral one-dimensional structure. There is only one 1,10-phenanthroline unit in the structure, which is bound to the $Sn^{II}$ and protrudes into the interchain spaces. The presence of the bulkier 1,10-phenanthroline molecules in **V** gives rise to zigzag chains (Figure 3, b). Neither compound **IV** nor **V** exhibit any significant hydrogen-bond interactions, probably because of the presence

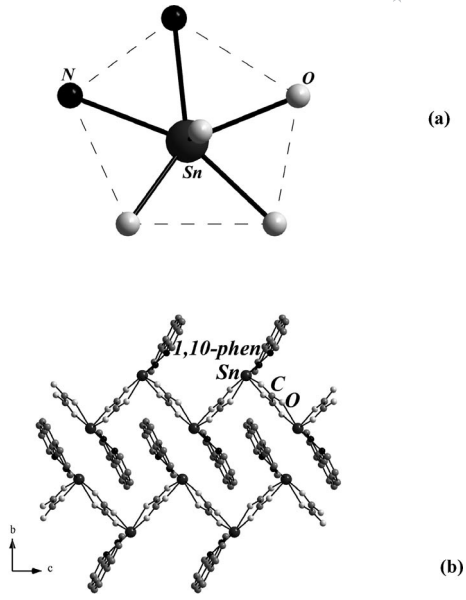


Figure 3. (a) The coordination environment around $Sn^{II}$ ions in $[C_{12}N_2H_8][SnC_2O_4]$ (**V**). (b) Structure of **V** in the *bc* plane showing the arrangement of chains. Note that the chains are arranged to maximize the π···π interactions (see text).

of the bulky ligands, 2,2′-bipyridine and 1,10-phenanthroline, bound to the $Sn^{II}$ ions and occupying the interchain spaces.

### Two-Dimensional Structure: $[C_5N_2H_{14}]_2[Sn_4(C_2O_4)_6]\cdot 7H_2O$ (VI)

The two-dimensional layered compound **VI** has been synthesized under mild conditions, and has been obtained as a single phasic compound. The asymmetric unit of **VI** contains 61 non-hydrogen atoms. There are four Sn atoms that are crystallographically independent. All Sn atoms are coordinated to six oxygen atoms with three Sn–O distances in the range 2.168(5)–2.412(5) Å, and three in the range 2.465(5)–2.526(5) Å. The O–Sn–O bond angles are in the range 65.19(2)–145.52(2)° (av. 92.38°) (Table S1). The tin atoms are connected to the carbon atoms through the oxygen bridges. Similar to compounds **IV** and **V**, the octahedral Sn has five oxygen atoms lying in a plane forming a pentagon, while the sixth oxygen atom and the lone pair of electrons form the two vertices, above and below the plane of the pentagon, resulting in a pseudopentagonal bipyramidal arrangement around the $Sn^{II}$ ions (Figure 4, a). The pentagonal bipyramids are arranged such that lone pairs of the neighboring $Sn^{II}$ point in opposite directions. Similar coordination environments for $Sn^{II}$ have been encountered earlier in $Sn^{II}$ oxalate structures.[16,18] The C–O and C–C distances of the oxalate groups are in the expected ranges. Selected bond lengths are listed in Table 2.

The structure of **VI** consists of macroanionic sheets of formula $[Sn_4(C_2O_4)_6]^{4-}$ with interlamellar $[C_5N_2H_{14}]^{2+}$ ions, which act as the charge compensating cations. In addition, the interlamellar regions also possess seven molecules of water. The $Sn^{2+}$ and oxalate ions are connected together,

  

giving rise to the extended two-dimensional structure with highly distorted 12-membered ring apertures (Figure 4, b). Similar perforated sheets have been observed earlier in $Sn^{II}$ oxalates.[16,18] The layers are stacked one over the other in an AAA... fashion (Figure 4, c). The protonated amine molecules occupy the interlamellar region. The disposition of the amine molecules is such that, in projection, the protonated homopiperazine appears to occupy the middle of the perforation formed by the 12-membered rings. The pores penetrate the sheets in a direction perpendicular to the plane of the sheet and give rise to a solid with unidimensional channels (about $5.82 \times 11.92$ Å; longest atom–atom contact distance not including the van der Waals radii). Similar arrangements have been observed before.[18]

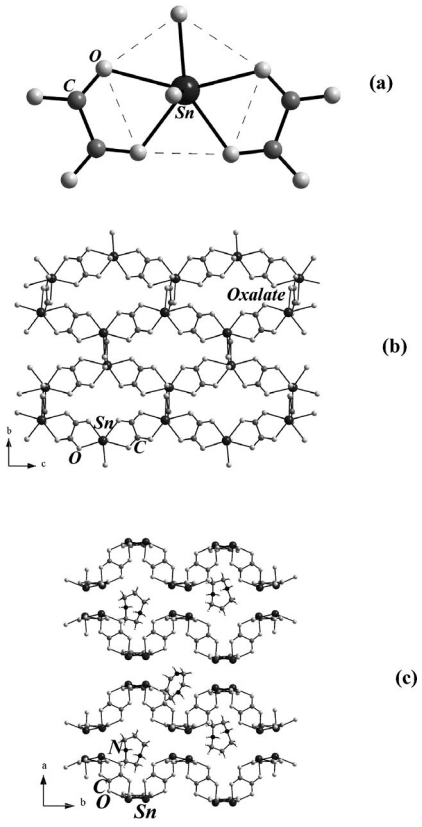


Figure 4. (a) The coordination environment around $Sn^{II}$ ions in $[C_5N_2H_{14}]_2[Sn_4(C_2O_4)_6]\cdot 7H_2O$ (**VI**). (b) Structure of **VI** in the *bc* plane, showing a single layer. Note that the 12-membered apertures are distorted. (c) Structure of **VI** in the *ab* plane showing the arrangement of the layers. The amine molecules and the water molecules (not shown) occupy the interlamellar region.

The presence of extraframework water molecules along with the protonated amine molecules in the interlamellar region gives rise to significant hydrogen-bond interactions in **VI**. Though we did not observe any O–H···O interactions, we have one N–H···O and several C–H···O interactions. The N···O (donor–acceptor) distance for the observable N–H···O interaction is 3.475(17) Å and the N–H···O bond angle is of the order of 166.0° and can be classified as a relatively weak hydrogen bond.[21] However, there are many C–H···O interactions and they appear to be significant. As mentioned earlier, the layered $Sn^{II}$ oxalate, **VI**, appears to be a good example to demonstrate the importance of C–H···O interactions in steering the solid-state assembly and directing the formation of the structure.[21] The observed C···O distances are in the range 2.762(9)–3.435(2) Å (av. 2.993Å), while the C–H···O bond angles are in the range 150.0–173.0° (av. 161.25°), all of which indicate reasonable hydrogen-bond interactions. It is clear that in **VI** the C–H···O interactions are dominant.

Six new tin oxalates **I**–**VI** have been synthesized by hydrothermal methods and their structures determined by single-crystal X-ray diffraction. Although all the compounds involve bonding between the oxalate units and $Sn^{2+}$ ions, they exhibit distinct differences. While **I**, **II**, and **III** are zero-dimensional, **IV** and **V** are one-dimensional, and **VI** has a two-dimensionally extended structure.

It is to be noted that the two zero-dimensional structures **I** and **II** have been formed employing the same organic ligand, 4,4′-bipyridine. The synthesis conditions employed for **I** and **II** are different; while **I** is formed in the presence of additional $H_3PO_4$ at a higher temperature (180 °C), **II** is formed at a lower temperature (150 °C). Comparing the synthesis conditions of **I** and **III**, the presence of excess oxalic acid seems necessary (Table S2). Structurally **I** and **III** are simple monomers, whereas **II** is a dimer. In the light of the formation of such simple structures, it is to be noted that the parent $Sn^{II}$ oxalate has a one-dimensional chain structure (Figure 5, a).[23] The starting $Sn^{II}$ oxalate does not dissolve normally at room temperature, and a combination of pH, pressure, and temperature plays a crucial role in breaking the chain into simpler building units (e.g., monomer, dimer, etc.), which then reassemble around the cations giving rise to the structures of **I**, **II**, and **III**. Such a dissolution and recrystallization mechanism has been suggested as one of the possible pathways for the formation of framework structures.[24]

The one-dimensional structures of **IV** and **V** have been prepared in the presence of 2,2′-bipyridine and 1,10-phenanthroline, respectively. In **IV**, 2,2′-bpy molecules bind selectively to only one of the $Sn^{II}$ ions (**IV**), whereas 1,10-phenanthroline binds to all the $Sn^{II}$ ions (**V**). This selective binding of the 2,2′-bpy ligand has resulted in two distinct types of coordination (four and six) for $Sn^{II}$ ions in **IV**, whereas only one type of coordination (six) is observed in **V**. We also observe the presence of a free 2,2′-bipyridine unit in between the chains, which is reflected in an increase of the interchain distance in **IV**, compared to **V**. The "*c*" lattice parameter in **IV** is about 5 Å longer than in **V**, though the structures of **IV** and **V** are comparable. The increase in the "*c*" parameter is approximately equivalent to the length of the 2,2′-bipyridine molecule. The structures of **IV** and **V** have comparable features to a previously reported one-dimensional tin(II) oxalate, $[C_5H_5N][SnC_2O_4]$[17] (Figure 5, b).

As the one-dimensional compounds **IV** and **V** have been prepared from a reaction mixture that contains $Sn^{II}$ oxalate, which itself is one-dimensional, it is pertinent to compare the 1D structures of **IV** and **V** with the parent $Sn^{II}$ oxalate

  

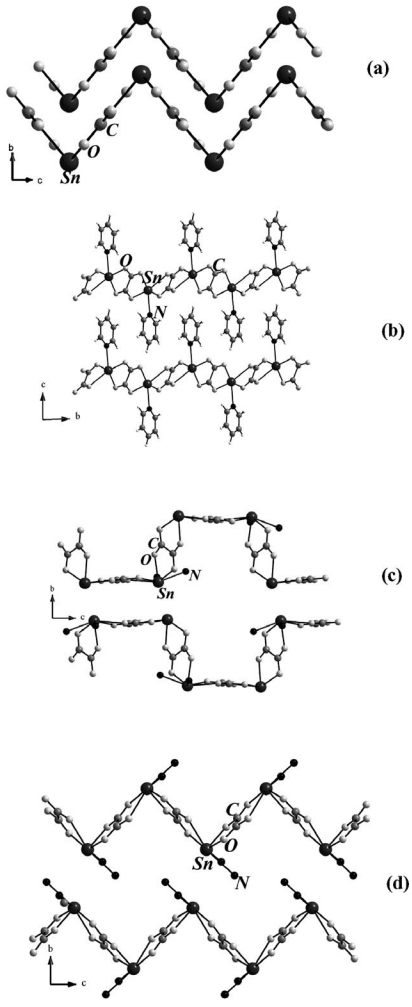


Figure 5. View of the one-dimensional $Sn^{II}$ oxalate structures in the *bc* plane. (a) The parent $Sn^{II}$ oxalate, $SnC_2O_4$, (b) $Sn^{II}$ oxalate with 5-coordinate $Sn^{II}$ atom, $[C_5H_5N][SnC_2O_4]$, (c) $[C_{10}N_2H_8]_2[Sn(C_2O_4)]_2$ (**IV**), and (d) $[C_{12}N_2H_8][SnC_2O_4]$ (**V**).

structure (Figure 5, a–d). In the starting $Sn^{II}$ oxalate, the $Sn^{II}$ ions are exclusively 4-coordinate with respect to the oxygen atoms, whereas both 4- and 6-coordination for Sn have been observed in the present compounds. The higher coordination of Sn, obviously, is due to the ligation by 2,2′-bpy and 1,10-phenanthroline molecules in **IV** and **V**, respectively. The compounds **IV** and **V**, as well as the parent $Sn^{II}$ oxalate, have a bent structure (zigzag) with a bend angle of about 79.1°. The interchain distance, however, varies between the three structures, with the largest distance observed in **IV**, because of the presence of the extra 2,2′-bipy between the chains (Figure S8). It has been observed that the $5s^2$ lone pair in $Sn^{II}$ compounds occupies a volume equivalent to that of an oxide ion $O^{2-}$ (about 11.98 $Å^3$).[25] As the lone pair occupies considerable volume, it is expected to create reasonable stress on the one-dimensional tin oxalate chains, which results in a zigzag arrangement.

Compound **VI** has a layered structure with features comparable to other two-dimensional $Sn^{II}$ oxalate structures reported in the literature.[18] As there are not many reports of bivalent oxalate structures available in the literature,[6,26] it is illustrative to compare the present structure with other bivalent oxalate structures. Thus, while **VI** shows comparable structural features with the $Sn^{II}$ oxalate, $[(CH_3)_2NH(CH_2)_2NH(CH_3)_2]^{2+}[Sn_2(C_2O_4)_3]^{2-}\cdot H_2O$,[18] it exhibits significant differences from other layered bivalent oxalates, for example, $[C_4N_2H_{12}][Zn_2(C_2O_4)_3]\cdot 4H_2O$[8] (Figure 6, a,b). The oxalate structures of bivalent elements (zinc and cobalt) are built up from the connectivity between the metal atoms and the oxalate units, forming near-perfect honeycomb layers. In the present structure, the honeycomb layers are highly distorted because of the presence of the bulky stereoactive lone pair of electrons of $Sn^{II}$. The lone pair manifests itself within the structure in such a way that the $Sn^{II}$ oxalate layers are not planar and the apertures are highly distorted.

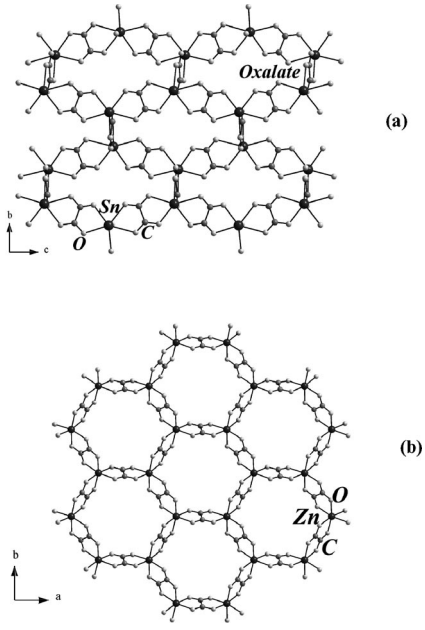


Figure 6. The two-dimensional bivalent oxalate structures, (a) $[C_5N_2H_{14}]_2[Sn_4(C_2O_4)_6]\cdot 7H_2O$ (**VI**) and (b) zinc(II) oxalate, $[C_4N_2H_{12}][Zn_2(C_2O_4)_3]\cdot 4H_2O$.

As mentioned earlier, the one-dimensional compounds, **IV** and **V**, do not possess any hydrogen-bond interactions. In the absence of such interactions, the structural stability might be due to the π···π interactions between the ligand amines, 2,2′-bpy and 1,10-phenanthroline. There has been considerable interest in the study of π···π interactions, especially in their role in the structural arrangement and stability in organic π-conjugated systems.[27,28] To evaluate and understand the nature of π···π interactions, we have carried out simple calculations. Our studies reveal that the π···π interactions between the various heterocyclic ligands are negligible, except in **V**. From the arrangement of the 1,10-phenanthroline molecules in **V**, one can expect favorable π···π interactions. We find that the centroid–centroid distance *d* between the 1,10-phenanthroline rings is 3.51 Å and the interplanar angle $\theta = 0.42°$. The interplanar angle ($\theta$), which is close to zero, indicates that the 1,10-phenanthroline rings

  

are arranged one over the other, but the stacking is in an antiparallel direction (Figure S7). This type of stacking is commonly observed in systems exhibiting dipolar properties. To understand the role of the π···π interactions, we have performed calculations using the AM1-parameterized Hamiltonian available in the Gaussian program suite.[29,31] AM1 methods, along with a semiclassical dipolar description, have been employed recently to establish the relationship between the stability and geometries of organic molecules.[32] From these calculations, the dipole moment of the 1,10-phenanthroline molecules was found to be 1.2 Debye; the dipole moment value for the stacked arrangement of the rings, however, was found to be zero. The antiparallel arrangement of the 1,10-phenanthroline molecules reduces the dipole–dipole repulsion and facilitates π-electron polarizations, which play an important role in the observed structural stability of **V**. The strength of the π···π interactions has also been evaluated based on single-point energy calculations, without the symmetry constraints, based on the crystal structure geometry. The π···π interaction energy was found to be in the range 5–6 kcal mol$^{-1}$, which is comparable to the intermediate hydrogen-bond strength (about 10 kcal mol$^{-1}$) in N–H···O and O–H···O systems.[21]

Compounds **I**, **II**, and **IV** present a unique situation because of the presence of aromatic molecules such as 4,4′-bpy (**I** and **II**) and 2,2′-bpy (**IV**) in between the tin(II) oxalate units. The presence of such aromatic ligands (π systems) can contribute to the stability through the lone-pair ($Sn^{II}$)–π orbital interactions. We have taken compounds **II** and **IV** as model systems for evaluating lone-pair interactions, and have employed natural bond orbital (NBO) analysis.[30,33] The minimum distances between the $Sn^{II}$ ions and the aromatic rings are 3.686 Å and 2.841 Å, for **II** and **IV**, respectively. These distances are less than the sum of the van der Waals radii of Sn and C (van der Waals radii of Sn and C are 2.17 Å and 1.70 Å, respectively). We have used a relativistically corrected effective core potential (ECP) of LANL2DZ for the Sn atom and a standard 6-31+g(d,p) basis for C, H, and N. Based on the NBO analysis, one observes a natural population of +1.17e on the $Sn^{II}$ ion and the rest on the ligand for **II**. For **IV**, the natural population is +1.31e on the $Sn^{II}$. The substantially lower positive charge on the Sn atom and the delocalized balance of charge of the aromatic ring are suggestive of reasonable interactions between the metal ion and the aromatic systems. The plots of the NBO orbitals for **II** and **IV** show interactions between the lone pair on Sn and π orbitals in the ring (Figure S9). The π* orbitals of the bipyridyl group are empty and can accept the lone pair of electrons from the $Sn^{II}$ atom.[34] Thus, the NBO calculations reveal that lone-pair/π interactions can also contribute towards the structural stability.

The formation of a hierarchy of structures in the family of $Sn^{II}$ oxalates indicates that it is possible to visualize the formation of such structures through a building-up process. It has been shown recently[35] that a monomeric zinc oxalate species progressively transforms to 1D, 2D, and 3D structures depending on the reaction conditions. Similarly, one can visualize the formation of higher-dimensional structures from simple monomer species.[36] The compounds **I**–**VI** have been prepared using $Sn^{II}$ oxalate as the starting material, which has a one-dimensional structure. It is clear that in all the cases the parent $Sn^{II}$ oxalate breaks down under the hydrothermal condition to form the simple monomeric $Sn^{II}$ oxalate units, which are then reassembled. Based on this view, a possible pathway for the formation of the various structures may be considered from the monomer (Figure S11). A mechanism of this kind is feasible as the pathway involves the addition or the removal of the oxalate or $Sn^{II}$ oxalate species progressively. Further work is required to correlate and understand the various factors that can play an important role in the formation of such structures.

## Conclusions

The synthesis of six new $Sn^{II}$ oxalates possessing a hierarchy of structures has been accomplished. The present solids represent examples illustrating the importance of weak intermolecular forces like hydrogen bonding, π stacking and lone-pair/π interactions in the synthesis and structural stability of lower-dimensional compounds. The isolation of new types of zero- and one-dimensional $Sn^{II}$ oxalates offers clues towards our understanding of the formation of complex structures within the family of oxalates. Our studies indicate that the lone pair of electrons plays an important role in the control of the formation of a particular structure.

## Experimental Section

**Synthesis:** Compounds **I**–**VI** were synthesized under hydrothermal conditions starting from a mixture containing tin(II) oxalate, oxalic acid, and an organic amine. The various synthesis conditions employed in the present study are presented in Table 3. In all the cases, the reaction mixtures were homogenized for about 30 min at room temperature and heated in a 23-mL PTFE-lined stainless steel acid digestion bomb for varying time periods and temperatures. The initial and final pH of the reaction mixtures, in all the cases, did not show any appreciable variation. The resulting products in **I**, **II**, **III**, and **IV** predominantly contained an unidentified white powder with a few isolated plate-like (**I**, **II**), needle-like (**III**), or block-like (**IV**) single crystals. The powder was found to be poorly crystalline and did not correspond to the structures of the accompanying compounds. In spite of our repeated attempts, we were not able to prepare the compounds in pure form and hence other than the single-crystal structure, we have not been able to characterize them completely (Table S2). However, in the case of **V** and **VI**, large quantities of block-like and needle-like crystals admixed with a small amount of white powder were obtained. The crystals were easily separated manually under the microscope for further studies and characterizations. In all the preparations, the products were washed with deionized water and dried at ambient conditions.

**Single-Crystal Structure Determination:** A suitable colorless single crystal of each compound was carefully selected and the single-crystal diffraction data were collected on a Bruker AXS Smart Apex CCD diffractometer at room temperature (293 K). The X-ray

  

Table 3. Synthesis conditions for compounds **I**–**VI**.

| No. | Synthesis condition | | | | Composition |
|---|---|---|---|---|---|
| | Mole ratio | Temp. [°C] | Time [h] | pH | |
| 1 | $SnC_2O_4/2H_3PO_4/1.5$(4,4′-bipy)$/167H_2O$ | 150 + 180 | 48 + 48 | 3.5 | $[C_{10}N_2H_{10}][Sn(C_2O_4)_2]$, **I** + unidentified phase |
| 2 | $SnC_2O_4/3$(4,4′-bipy)$/167H_2O$ | 150 + 180 | 48 + 48 | 5.0 | $[C_{10}N_2H_{10}][Sn_2(C_2O_4)_3]$, **II** + unidentified phase |
| 3 | $SnC_2O_4/4H_2C_2O_4/1.5$BAPEN$/167H_2O$ | 150 + 180 | 48 + 24 | 7.0 | $[C_8N_4H_{26}][Sn(C_2O_4)_2]_2{\cdot}2H_2O$, **III** + unidentified phase |
| 4 | $SnC_2O_4/4H_2C_2O_4/1.5$BAPEN$/1H_3PO_4/167H_2O$ | 150 + 180 | 48 + 24 | 4.0 | $[C_8N_4H_{26}][Sn(C_2O_4)_2]_2{\cdot}2H_2O$, **III** + unidentified phase |
| 5 | $SnC_2O_4/1H_3PO_4/1$(2,2′-bipy)$/278H_2O$ | 150 + 180 | 48 + 48 | 4.0 | $[C_{10}N_2H_8]_2[Sn(C_2O_4)]_2$, **IV** + unidentified phase |
| 6 | $SnC_2O_4/1.0H_3PO_4/3$(1,10-phen)$/167H_2O$ | 150 + 180 | 48 + 48 | 3.0 | $[C_{12}N_2H_8][SnC_2O_4]$, **V** |
| 7 | $2SnC_2O_4/1$HOMOPIP$/110H_2O$ | 125 | 48 | 6.0 | $[C_{10}N_4H_{28}][Sn_4(C_2O_4)_6]{\cdot}7H_2O$, **VI** |

Table 4. Crystal data and structure refinement parameters for compounds **I**–**VI**.[a]

| | **I** | **II** | **III** | **IV** | **V** | **VI** |
|---|---|---|---|---|---|---|
| Empirical formula | $C_{14}H_{10}N_2O_8Sn$ | $C_{13}H_{10}N_2O_6Sn$ | $C_8H_{15}N_2O_9Sn$ | $C_{24}H_{16}N_4O_8Sn_2$ | $C_{14}H_8N_2O_4Sn$ | $C_{22}H_{28}N_4O_{31}Sn_4$ |
| Formula mass | 452.93 | 408.92 | 401.91 | 725.80 | 386.91 | 1319.24 |
| Crystal system | monoclinic | triclinic | triclinic | monoclinic | monoclinic | monoclinic |
| Space group | $C2_1/c$ (no. 15) | $P\bar{1}$ (no. 2) | $P\bar{1}$ (no. 2) | $P2_1/c$ (no. 14) | $P2_1/c$ (no. 14) | $P2_1/c$ (no. 14) |
| Crystal size [mm] | $0.20\times0.10\times0.08$ | $0.20\times0.12\times0.10$ | $0.16\times0.08\times0.06$ | $0.14\times0.12\times0.08$ | $0.12\times0.10\times0.08$ | $0.18\times0.08\times0.06$ |
| $a$ [Å] | 13.839(9) | 7.4500(15) | 6.3035(11) | 10.170(2) | 9.6764(19) | 16.954(6) |
| $b$ [Å] | 5.179(3) | 9.1380(18) | 7.6671(14) | 16.232(4) | 16.407(3) | 20.500(7) |
| $c$ [Å] | 21.720(14) | 11.140(2) | 14.162(3) | 14.686(3) | 8.9254(18) | 11.693(4) |
| $\alpha$ [°] | 90 | 102.197(3) | 88.232(3) | 90 | 90 | 90 |
| $\beta$ [°] | 103.445(9) | 106.850(3) | 79.512(3) | 93.767(4) | 113.391(3) | 96.061(6) |
| $\gamma$ [°] | 90 | 92.178(3) | 82.416(3) | 90 | 90 | 90 |
| $V$ [Å$^3$] | 1514.2(17) | 705.4(2) | 667.1(2) | 2419.0(9) | 1300.6(4) | 4041(2) |
| $Z$ | 4 | 2 | 2 | 4 | 4 | 4 |
| Temp. [K] | 293 | 293 | 293 | 293 | 293 | 293 |
| $\rho_{calcd}$ [g cm$^{-3}$] | 1.987 | 1.925 | 2.001 | 1.996 | 1.976 | 2.168 |
| $\mu$ [mm$^{-1}$] | 1.737 | 1.843 | 1.962 | 2.124 | 1.982 | 2.553 |
| Wavelength [Å] | 0.71073 | 0.71073 | 0.71073 | 0.71073 | 0.71073 | 0.71073 |
| $\theta$ range [°] | 1.93–27.94 | 1.96–28.03 | 2.68–27.98 | 1.87–28.06 | 2.48–28.07 | 1.56–28.07 |
| Collected reflections | 6023 | 8242 | 5810 | 20753 | 14738 | 34615 |
| Unique reflections | 1757 | 3272 | 3024 | 5714 | 3091 | 9457 |
| Parameters | 114 | 199 | 189 | 344 | 190 | 550 |
| Goodness of fit | 1.103 | 1.119 | 1.063 | 1.036 | 1.149 | 1.135 |
| $R$ index [$I > 2\sigma(I)$] | $R_1 = 0.0324$, $wR_2 = 0.0749$ | $R_1 = 0.0222$, $wR_2 = 0.0544$ | $R_1 = 0.0213$, $wR_2 = 0.0506$ | $R_1 = 0.0405$, $wR_2 = 0.0708$ | $R_1 = 0.0235$, $wR_2 = 0.0580$ | $R_1 = 0.0557$, $wR_2 = 0.1120$ |
| $R$ (all data) | $R_1 = 0.0371$, $wR_2 = 0.0770$ | $R_1 = 0.0248$, $wR_2 = 0.0557$ | $R_1 = 0.0235$, $wR_2 = 0.0517$ | $R_1 = 0.0755$, $wR_2 = 0.0815$ | $R_1 = 0.0285$, $wR_2 = 0.0602$ | $R_1 = 0.0816$, $wR_2 = 0.1208$ |
| Largest diff. peak and hole [e Å$^{-3}$] | 0.946 and –0.634 | 0.295 and –0.498 | 0.490 and –0.276 | 0.626 and –0.717 | 0.334 and –0.958 | 1.419 and –1.606 |

[a] $R_1 = \Sigma||F_o| - |F_c||/\Sigma|F_o|$; $wR_2 = \{\Sigma[w(F_o^2 - F_c^2)]/\Sigma[w(F_o^2)^2]\}^{1/2}$; $w = 1/[\rho^2(F_o)^2 + (aP)^2 + bP]$; $P = [\max(F_o)^2 + 2(F_c)^2]/3$, where $a$ = 0.0417 and $b$ = 0.7807 for **I**, $a$ = 0.0271 and $b$ = 0.1818 for **II**, $a$ = 0.0248 and $b$ = 0.3628 for **III**, $a$ = 0.0254 and $b$ = 1.8879 for **IV**, $a$ = 0.0281 and $b$ = 0.5440 for **V**, and $a$ = 0.0307 and $b$ = 23.0260 for **VI**.

generator was operated at 50 kV and 35 mA using Mo-$K_\alpha$ ($\lambda$ = 0.71073 Å) radiation. Data were collected with $\omega$-scans of width 0.3°. A total of 606 frames were collected in three different settings of $\phi$ (0, 90, and 180°), keeping the sample-to-detector distance fixed at 6.03 cm and the detector position fixed at –25°. Pertinent experimental details of the structure determination are listed in Table 4.

The data were reduced using SAINTPLUS[37] and an empirical absorption correction was applied using the SADABS program.[38] The crystal structure was solved and refined by direct methods using SHELXL-97 present in the WinGx suite of programs.[39] The hydrogen positions were initially located in the difference Fourier maps, and for the final refinement the hydrogen atoms were placed in geometrically ideal positions and refined using the riding mode. The lattice water molecules in **VI** were found to be disordered, which precluded the location of the hydrogen positions. Because of the disorder, we have employed isotropic refinement for the water molecules. The last cycles of refinements included all the atomic positions, anisotropic thermal parameters for all the non-hydrogen atoms, and isotropic thermal parameters for all the hydrogen atoms. Full-matrix least-squares structure refinement against $|F|^2$ was carried out using the WinGx suite of programs.[39]

CCDC-629169 (for **I**), -629170 (for **II**), -629171 (for **III**), -629172 (for **IV**), -629173 (for **V**), and -629174 (for VI) contain the supplementary crystallographic data for this paper. These data can be obtained free of charge from The Cambridge Crystallographic Data Centre via www.ccdc.cam.ac.uk/data_request/cif.

**Initial Characterizations:** The two pure $Sn^{II}$ oxalates, **V** and **VI**, were characterized using powder X-ray diffraction (XRD) (Figure S1, S4), infrared spectroscopy (IR) (Figure S2, S5), thermogravimetric analysis (TGA) (Figure S3, S6), and elemental analysis. TGA studies were performed in flowing oxygen (flow rate =

  

100 mL min$^{-1}$) in the temperature range 30–800 °C (heating rate = 5 °C min$^{-1}$; Mettler-Toledo, TG850). Infrared spectra (IR) were recorded in the range 400–4000 cm$^{-1}$ using the KBr pellet method (Perkin–Elmer, SPECTRUM 1000). The powder X-ray diffraction pattern was recorded on crushed single crystals in the $2\theta$ range 5–50° using Cu-$K_\alpha$ radiation (Philips, X'pert Pro). The XRD patterns indicated that the products were new and entirely consistent with the simulated XRD patterns obtained from the single-crystal structures. Elemental analysis of the compounds was carried out using atomic absorption spectroscopy (ThermoFinnigan Flash EA 1112 CHNS analyzer). The C, H, and N analyses of **V** and **VI** are as follows. **V**: calcd. C 43.42, H 2.07, N 7.24; found C 43.01, H 1.98, N 7.11; **VI**: calcd. C 19.81, H 3.15, N 4.20; found C 19.19, H 2.96, N 3.92.

The IR spectra of **V** and **VI** show similar features (Figure S2, S5). The following bands (cm$^{-1}$) have been observed, for **V**: $\nu_s$(C–H) = 2919, $\delta_s$ (C–H) = 1509, $\nu_{as}$(CO) = 1661, $\nu_s$(CO) = 1423, $\nu_s$(O–C–O) = 1342, 1290, $\delta$(O–C–O) = 840, 781, $\nu_s$(C–C) = 1238, and for **VI**: $\nu_s$(O–H) = 3555, $\nu_s$(N–H) = 3024, $\delta$(N–H) = 1878, $\nu_s$(C–H) = 2806, $\nu_{as}$(CO) = 1619, $\nu_s$(CO) = 1421, $\nu_s$(O–C–O) = 1348 cm$^{-1}$, 1298, $\delta$(O–C–O) = 895, 787, $\nu_s$(C–C) = 1358.

The results of the TGA studies indicated two weight losses for both the compounds (Figure S3, S6). For **V**, a sharp weight loss in the region 250–300 °C was followed by a tail between 350–425 °C. For **VI**, an initial weight loss around 100 °C was followed by a sharp loss in the region 250–300 °C. The total observed weight losses for **V** and **VI** were 60.01% and 56.12%, respectively. The weight loss corresponded to the loss of the amine and oxalate units for **V** (calcd. 61.1%) and to the loss of lattice water, amine, and the oxalate units for **VI** (calcd. 59.03%). The final products, in both the cases, were found to be poorly crystalline, as found by powder XRD, and the majority of the XRD lines corresponded to the crystalline phase $SnO_2$ (JCPDS: 00-005-0467).

**Supporting Information** (see footnote on the first page of this article): Powder XRD patterns, IR spectra and TGA curves for compounds **V** and **VI**, along with the stacking diagram of 1,10-phen rings for compound **V**; figures of the coordination geometries around the central $Sn^{II}$ atom in compounds **I**–**VI**, the NBO plots for compounds **II** and **IV**, as well as the electron-density plot for compound **I**; a schematic representation of a possible pathway for the formation of the various tin oxalate species starting from the monomer, as well as the details of the DFT calculations for the π···π interactions; selected bond angles for compounds **I**–**VI**; details of the synthesis conditions.

## Acknowledgments

The authors thank the reviewers for their many helpful suggestions. S. N. thanks the Council of Scientific and Industrial Research for the award of a research grant and the authors thank DST-IRPHA for the BRUKER-CCD facility. S. N. also thanks the Department of Science and Technology (DST), Government of India, for the award of a RAMANNA fellowship.

[1] A. K. Cheetham, T. Loiseau, G. Ferey, *Angew. Chem. Int. Ed.* **1999**, *38*, 3268–3292.
[2] S. Natarajan, *Proc. Ind. Acad. Sci. (Chem. Sci.)* **2000**, *112*, 249–272.
[3] a) D. Maspoch, D. Ruiz-Molina, J. Vaciana, *Chem. Soc. Rev.* **2007**, *36*, 770–818; b) G. Ferey, *Chem. Soc. Rev.* **2008**, *37*, 191–214.
[4] C. N. R. Rao, S. Natarajan, R. Vaidyanathan, *Angew. Chem. Int. Ed.* **2004**, *43*, 1466–1496, and references therein.
[5] a) Y.-Q. Sun, J. Zhang, G.-Y. Yang, *Dalton Trans.* **2003**, *18*, 3634–3638; b) D. J. Price, A. K. Powell, P. T. Wood, *Dalton Trans.* **2003**, *12*, 2478–2482; c) S. Decurtins, H. Schmalle, R. Pellaux, *New J. Chem.* **1998**, *2*, 117–121.
[6] a) R. Pellaux, H. W. Schmalle, S. Decurtins, P. Fischer, F. Fauth, B. Ouladdiaf, T. Hauss, *Physica B* **1997**, *234*, 783–784; b) M. Clemente-Leon, E. Coronado, J. R. Galan-Mascaros, C. J. Gomez-Garcia, *Chem. Commun.* **1997**, *18*, 1727–1728; c) S. G. Carling, C. Mathoniere, P. Day, K. M. A. Malik, S. J. Coles, M. B. Hursthouse, *J. Chem. Soc. Dalton Trans.* **1996**, 1839–1843; d) E. Coronado, J. R. Galan-Mascaros, C. J. Gomez-Garcia, J. M. Martinez-Agudo, *Adv. Mater.* **1999**, *11*, 558–561; e) C. J. Nuttall, P. Day, *Chem. Mater.* **1998**, *10*, 3050–3057.
[7] C. N. R. Rao, J. Gopalakrishnan, *New Directions in Solid State Chemistry*, Cambridge University Press, Cambridge, UK, **1986**.
[8] R. Vaidyanathan, S. Natarajan, C. N. R. Rao, *J. Chem. Soc. Dalton Trans.* **2001**, *5*, 699–706.
[9] C. N. R. Rao, S. Natarajan, A. Choudhury, S. Neeraj, A. A. Ayi, *Acc. Chem. Res.* **2001**, *34*, 80–87.
[10] C. N. R. Rao, S. Natarajan, S. Neeraj, *J. Am. Chem. Soc.* **2000**, *122*, 2810–2817.
[11] R. Vaidhyanathan, S. Natarajan, C. N. R. Rao, *J. Mol. Struct.* **2002**, *608*, 123–133.
[12] P. A. Prasad, S. Neeraj, S. Natarajan, C. N. R. Rao, *Chem. Commun.* **2000**, *14*, 1251–1252.
[13] R. Vaidyanathan, S. Natarajan, C. N. R. Rao, *Chem. Mater.* **2001**, *13*, 185–191.
[14] R. Vaidyanathan, S. Natarajan, C. N. R. Rao, *Inorg. Chem.* **2002**, *41*, 4496–4501.
[15] S. Si, C. Li, R. Wang, Y. Li, *J. Coord. Chem.* **2006**, *59*, 215–222.
[16] S. Ayyappan, A. K. Cheetham, S. Natarajan, C. N. R. Rao, *Chem. Mater.* **1998**, *10*, 3746–3755.
[17] T. O. Salami, K. Marouchkin, P. Y. Zavalij, S. R. J. Oliver, *Chem. Mater.* **2002**, *14*, 4851–4857.
[18] S. Natarajan, R. Vaidyanathan, C. N. R. Rao, S. Ayyappan, A. K. Cheetham, *Chem. Mater.* **1999**, *11*, 1633–1639.
[19] F. A. Cotton, G. Wilkinson, C. A. Murillo, M. Bochmann, *Advanced Inorganic Chemistry*, 6th ed., Wiley Interscience Publication, **2003**..
[20] W. J. Moore, L. Pauling, *J. Am. Chem. Soc.* **1941**, *63*, 1392–1394.
[21] L. Brammer, *Hydrogen Bonds in Inorganic Chemistry: Application to Crystal Design*, in *Crystal Design: Structure and Function* (Ed.: G. R. Desiraju), John Wiley & Sons, Chichester, UK, **2003**, pp. 1–76.
[22] G. R. Desiraju, T. Steiner, *The Weak Hydrogen Bond: In Structural Chemistry and Biology*, Oxford University Press, Oxford, New York, **1999**.
[23] A. D. Christie, R. A. Howie, W. Moser, *Inorg. Chim. Acta* **1979**, *36*, L447–L448.
[24] A. A. Ayi, A. Choudhury, S. Natarajan, S. Neeraj, C. N. R. Rao, *J. Mater. Chem.* **2001**, *4*, 1181–1191.
[25] S. Andersson, A. Aström, Natl. Bur. Stand. US, Spec. Publ. 364, Solid State Chem. Proc. 5th Mater. Res. Symp., **1972**, p. 3.
[26] a) O. R. Evans, W. Lin, *Cryst. Growth Des.* **2001**, *1*, 9–11; b) S. Natarajan, *Solid State Sci.* **2002**, *10*, 1331–1342; c) R. Vaidyanathan, S. Natarajan, C. N. R. Rao, *J. Solid State Chem.* **2002**, *167*, 274–281.
[27] C. A. Hunter, J. K. M. Sanders, *J. Am. Chem. Soc.* **1990**, *112*, 5525–5534.
[28] C. A. Hunter, J. Singh, J. K. M. Sanders, *J. Mol. Biol.* **1991**, *218*, 837–846.
[29] M. J. Frisch, G. W. Trucks, H. B. Schlegel, G. E. Scuseria, A. Robb, J. R. Cheeseman, J. A. Montgomery Jr, T. Vreven, K. N. Kudin, J. C. Burant, J. M. Millam, S. S. Iyengar, J. Tomasi, V. Barone, B. Mennucci, M. Cossi, G. Scalmani, N. Rega, G. A.

  

Petersson, H. Nakatsuji, M. Hada, M. Ehara, K. Toyota, R. Fukuda, J. Hasegawa, M. Ishida, T. Nakajima, Y. Honda, O. Kitao, H. Nakai, M. Klene, X. Li, J. E. Knox, H. P. Hratchian, J. B. Cross, C. Adamo, J. Jaramillo, R. Gomperts, R. E. Stratmann, O. Yazyev, A. J. Austin, R. Cammi, C. Pomelli, J. W. Ochterski, P. Y. Ayala, K. Morokuma, G. A. Voth, P. Salvador, J. J. Dannenberg, V. G. Zakrzewski, S. Dapprich, A. D. Daniels, M. C. Strain, O. Farkas, D. K. Malick, A. D. Rabuck, K. Raghavachari, J. B. Foresman, J. V. Ortiz, Q. Cui, A. G. Baboul, S. Clifford, J. Cioslowski, B. B. Stefanov, G. Liu, A. Liashenko, P. Piskorz, I. Komaromi, R. L. Martin, D. J. Fox, T. Keith, M. A. Al-Laham, C. Y. Peng, A. Nanayakkara, M. Challacombe, P. M. W. Gill, B. Johnson, W. Chen, M. W. Wong, C. Gonzalez, J. A. Pople, *Gaussian 03*, Revision B.05, Gaussian, Inc., Pittsburgh, PA, **2003**.

[30] S. F. Boys, F. Bernardi, *Mol. Phys.* **1970**, *19*, 553.

[31] M. J. S. Dewar, E. G. Zoebisch, E. F. Healy, J. J. P. Stewart, *J. Am. Chem. Soc.* **1985**, *107*, 3902–3909.

[32] A. Dutta, S. K. Pati, *J. Chem. Phys.* **2003**, *118*, 8420–8427.

[33] a) G. A. DiLabio, E. R. Johnson, *J. Am. Chem. Soc.* **2007**, *129*, 6199–6203; b) M. Egli, S. Sarkhel, *Acc. Chem. Res.* **2007**, *40*, 197–205.

[34] R. Ahuja, A. G. Samuelson, *Cryst. Eng. Commun.* **2003**, *5*, 395–399.

[35] M. Dan, C. N. R. Rao, *Angew. Chem. Int. Ed.* **2005**, *45*, 281–285.

[36] C. N. R. Rao, S. Natarajan, A. Choudhury, S. Neeraj, A. A. Ayi, *Acc. Chem. Res.* **2001**, *34*, 80–87.

[37] *SMART (V 5.628), SAINT (V 6.45a), XPREP and SADABS*, Bruker AXS Inc., Madison, WI, USA, **2004**.

[38] G. M. Sheldrick, *SADABS Siemens Area Detector Absorption Correction Program*, University of Göttingen, Göttingen, Germany, **1994**.

[39] Crystallographic Program for Microsoft Windows®, *WinGx V 1.64.05*, **2003**.

Received: July 12, 2007
Published Online: January 31, 2008

  